Hindawi
Shock and Vibration
Volume 2019, Article ID 5392930, 14 pages
https://doi.org/10.1155/2019/5392930

Research Article

A Fast Modeling Technique for the Vertical Train-Track-Bridge Interactions

Hanyun Liu,[1] **Zhiwu Yu**,[1,2] **and Wei Guo**[1,2]

[1]*School of Civil Engineering, Central South University, Changsha 410075, China*
[2]*National Engineering Laboratory for High-Speed Railway Construction, Changsha 410075, China*

Correspondence should be addressed to Wei Guo; guowei@csu.edu.cn

Received 29 January 2019; Revised 19 March 2019; Accepted 31 March 2019; Published 28 April 2019

Academic Editor: Jean-Jacques Sinou

Copyright © 2019 Hanyun Liu et al. This is an open access article distributed under the Creative Commons Attribution License, which permits unrestricted use, distribution, and reproduction in any medium, provided the original work is properly cited.

This paper proposed a fast modeling technique (FMT) for the vertical dynamic analysis of the coupled train-track-bridge (TTB) systems, which combines the train subsystems and track-bridge subsystems by the client-server technique to complete the entire TTB analysis on simplex OpenSees simulation platform. Thus, the FMT could dramatically reduce the time consumed of programming and modeling and significantly reduce the amount of data transmission between subsystems for TTB interaction. Moreover, FMT could take full advantage of OpenSees in nonlinear and seismic analysis. So FMT is a practical and convenient approach to analyze the TTB coupling vibration, and especially it is suitable for the junior researchers of TTB interaction. FMT could improve the modeling efficiency to save time.

1. Introduction

With the rapid development of high-speed railway over the past decades around the world, there have been numerous studies on the train-track-bridge (TTB) interaction problem, and the theory of TTB analysis is becoming mature [1–3]. From the perspective of efficiency, the TTB interaction dynamic analysis can be divided into the computational efficiency and modeling efficiency. There is much literature that focuses on improving computational efficiency, which includes new numerical algorithms and simulation methods, e.g., Zhai [4, 5] presented a fast explicit two-step method and a new family of predictor-corrector integration algorithm, Zhu et al. [6, 7] proposed a multi-time-step algorithm, Yang et al. [8, 9] used dynamic condensation method (DCM), and Xia utilized the mode superposition method (MSM) to solve the problem of coupled TTB systems; nevertheless, there is little literature addressed on how to enhance the modeling efficiency of the TTB systems.

Current various analytical methods for solving the TTB coupling vibration problem either have their shortcomings or are cumbersome and inconveniences for junior researchers or engineers in modeling. For example, the early analytic or semianalytic method [8–11] is suitable for the simplified model of a moving load, mass, or single-suspension vehicle across a simply supported beam bridge, and it does not effectively consider the coupling effect between the train and the bridge, so today it is rarely used in the analysis of large or actual TTB interaction. And the dynamic condensation method (DCM) [8, 9], the mode superposition method (MSM) [12–14], and the strongly coupled algorithms (SCA) [1, 15], also known as the direct integration method [12, 16–18], which treats the train, track, bridge as a single integrated system and solves the equation of motions of the TTB systems at each time step without any iteration, usually require researchers to write code by themselves. Therefore, it needs a researcher to have both deep programming skills and enough theoretical basis of TTB systems. Likewise, another frequently used analysis way, the loosely coupled iterative algorithms (LCA) [15], also known as the separation-iteration method [19, 20], needs investigators to master the multiple finite element analysis (FEA) software because the LCA partitions the TTB interaction system into a train subsystem and a track-bridge

subsystem, and then the train subsystem is simulated in multibody dynamics software like SIMPACK and UM or in MATLAB, and the track-bridge substructure is modeled in commercial general FEA software like ANSYS and ABAQUS or in MATLAB, for example, Cui [21] and Li et al. [22] combined SIMPACK with ANSYS to calculate the TTB coupling vibration response, Auciello et al. [23] and Hou et al. [24] combined SIMPACK with MATLAB to simulate the TTB systems, and Zhu et al. [6, 7] combined MATLAB with ANSYS to analyze the TTB interaction. In sum, the abovementioned analysis methods of the TTB interaction system require researchers to master at least one or two kinds of software and high programming ability, which is precisely a relatively difficult ability to improve for junior researchers and engineers. Therefore a convenient, efficient, and timesaving modeling approach to analyze the TTB interaction system is urgently needed.

Hence, this paper proposed a fast modeling technique (FMT) for the dynamic analysis of coupled TTB systems using the client-server technique [25] achieved in the OpenSees [26, 27] simulation platform. Compared with the SCA [6, 15], DCM [8, 9], and MCM [12–14], the amount of programming work of the FMT is very little. Meanwhile, compared to the LCA [6, 15] and MCM, the FMT just needs the investigators to grasp the OpenSees software, which is easy to learn and use. And the FMT has no additional work, namely, it does not need to export and import the modal parameters of the track-bridge subsystem or to repeatedly release and reload the model of two subsystems. Therefore, the presented method will dramatically reduce the time consumption for both programming and modeling and significantly reduce the amount of data transmission between the train and track-bridge subsystem in the TTB interaction problem. In addition, the FMT can handle nonlinear problems conveniently, e.g., the seismic analysis and nonlinear suspension, and is flexible, e.g., the displacement correction of the beam element under wheelset position could be handily considered to improve the computational accuracy of the wheel/rail contact force. FMT is efficient in modeling, yet there is no advantage in computational efficiency. The accuracy and practicability of the proposed method are validated and illustrated by some numerical examples.

2. Fast Modeling Technique (FMT)

2.1. Description of the FMT. The schematic diagram of the fast modeling technique (FMT) of the TTB interaction system is described in Figure 1. In the FMT, the TTB system is partitioned into train subsystem and track-bridge subsystem, which both are modeled in OpenSees and packaged as two servers. The wheel/rail interaction relation, which is used to confirm the compatibility of the forces and displacements at the contact point between the train and the track [5, 6], is handled as a client, which is a tiny piece of code written by TCL language. And the client uses the network communication technique to interconnect the two subsystems/servers. It is worth noting that the client and servers are all written with TCL language, which is the official language of OpenSees software. Then the entire TTB dynamic analysis process can be achieved in simplex OpenSees software. The OpenSees [28] is powerful and easy to learn and use. So, even junior researchers can quickly perform modeling and analysis of the train-track-bridge interaction. Otherwise, the advantages of OpenSees, such as its efficient nonlinear seismic analysis capabilities, abundant material and elemental libraries, and various numerical integration and iteration algorithms, could be quickly and fully utilized in TTB analysis.

The entire process of FMT can be described as follows. First, the train subsystem and track-bridge subsystem are established in OpenSees separately. Each subsystem numerical model is then packed as a server. The server is persistent in memory and performs the dynamic calculation. Note that the server needs to run the gravity load analysis in the beginning. Second, the server carries out one step dynamic analysis after receiving the client instruction. After that, the server goes into a waiting state until it receives the next command from the client. Meanwhile, the client runs with an assumptive initial boundary condition at the onset. Then, in each calculation step, the servers exchange data with the client; the client organizes data from the servers and sends the instruction to the servers. And the client is responsible for performing the convergence test and updating the stiffness matrix. The detailed steps of building the client and server's sockets are described in the literature [25].

The advantages of the FMT approach are as follows. (i) Convenient and fast modeling: to model in simplex OpenSees software, it is easy to implement. (ii) Efficient data transmission: the server is persistent in memory of OpenSees; thus, it does not require repeated reloading, releasing, and transmitting the model data; only the load data and boundary condition data need to be transmitted. (iii) Nonlinear and flexibility: to make full use of the OpenSees advantages. Therefore, the presented method is suitable for TTB coupling vibration analysis.

2.2. Train, Track, and Bridge Models. To describe the FMT in simple words, this paper just considers the two-dimensional TTB systems. For the three-dimensional TTB systems, the principle is the same, except that the client becomes more complicated in the processing of wheel/rail contact relationship, which needs to consider the role of tangential creep force. And this part work is in progress.

In this paper, the train subsystem is modeled with the multi-rigid body, which is composed of a body, two bogies, and four wheelsets [5, 29]. The wheelset considers only the vertical bouncing motion, while the body and two bogies consider the bouncing and pitch motion. So, the total degree of freedoms (DOFs) of the single train model is 10. The components between the bogie and its wheelsets and those between the car body and each bogie are connected by the linear or nonlinear springs and dampers.

The track and bridge models depend on the particular configuration of the track-bridge system. According to the

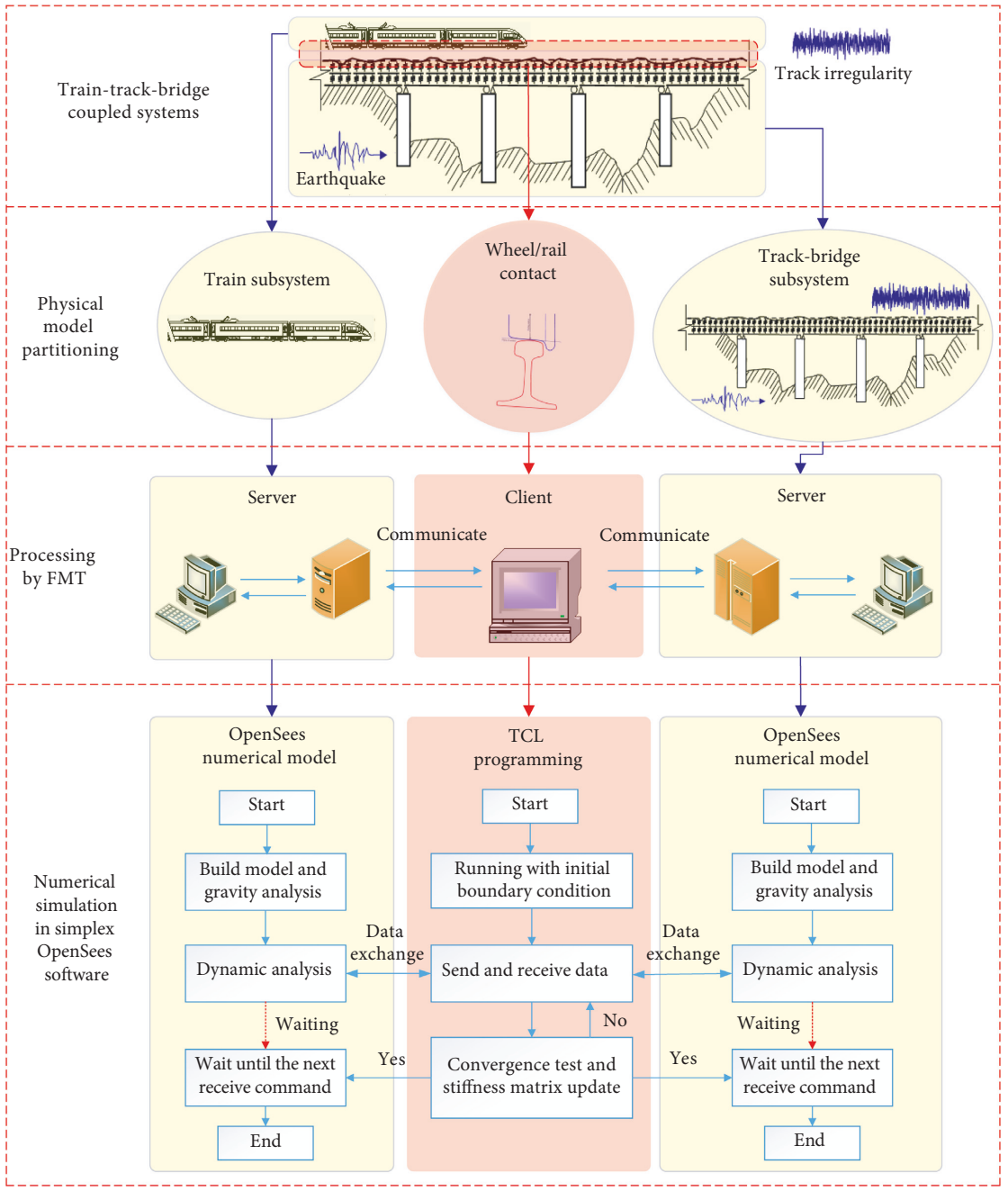

Figure 1: Schematic diagram of the proposed method for the train-track-bridge interaction system.

actual structure, the type of modeling element is different. The commonly used element types have a beam, truss, link, shell, and so on. The beam elements are often utilized for rails, track slabs, the main girders, piers, and piles, the truss and link elements are frequently used for fasteners, concrete asphalt mortar layer, bear, etc., and the shell elements are commonly used for the bridge deck [1, 6, 15].

The aforementioned train, track, and bridge subsystem are all modeled using the OpenSees FEA software. OpenSees provides a powerful library of elements and materials, such as the displacement-based beam element, force-based beam element, multiaxial cyclic plasticity material [28]. Therefore, researchers do not need to derive cumbersome formulas and dynamical matrix parameters of the TTB systems, such as the mass, damping, and stiffness matrix, and could directly build the TTB model in OpenSees. In addition, the effect of the track's random irregularity excitation is considered in the track-bridge model.

2.3. Wheel/Rail Constraint Relationship. This section mainly clarifies the wheel/rail relationship and deduces the wheel/rail constraint equation. In fact, when the concentrated force exerts on the beam element, the vertical actual displacement

u_1 of the load point consists of two portions: the interpolation displacement u_2 and the correction displacement u_3, as shown in Figure 2(a). The displacement u_2 interpolates from the nodal displacement of beam endpoint using the shape function [8, 9, 29]. And the correction displacement u_3 comes from the wheel/rail interaction force, which is beyond the displacement prescribed by the element's shape function. This item is rarely considered in most train-track-bridge models [5, 9, 12, 29], but it has a noteworthy effect in the wheel/rail contact force. In this paper, considering the influence of correction displacement item and track irregularity, the accuracy contact geometric relationship between the wheel and rail is shown in Figure 2(b).

In Figure 2(b), the ith wheelset is located on the rail beam element with length L_i. The distance of the wheelset to left endpoint of the rail beam element is x_i. And the wheelset bouncing displacement is denoted as $u_{w,i}$. The random track irregularity value is called $r_{w,i}$. $\delta_{w,i}$ denotes the penetration value between the wheel and the rail, which takes different values according to the selected normal contact model of the wheel and rail. For sticking contact model, $\delta_{w,i}$ is equal to zero; for sliding and separating contact model, $\delta_{w,i}$ is no less than zero. $u_{bc,i}$ denotes the rail vertical interpolation displacement at the contact point using the Hamilton cubic interpolation shape function [29]. $u_{s,i}$ denotes the correction displacement due to the wheelset's concentrated force. Then accurate wheel/rail contact relationship can be obtained.

According to Figure 2(b), the geometric coordination relationship between wheel and rail is written as

$$u_{w,i} = u_{bc,i} + u_{s,i} + \delta_{w,i} + r_{w,i}, \tag{1}$$

where $i = 1, \ldots, n$, n is the number of the wheelset. Equation (1) is rewritten in matrix form as

$$\mathbf{U}_w = \mathbf{U}_{bc} + \mathbf{U}_s + \Delta\mathbf{U} + \mathbf{R}, \tag{2}$$

where $\mathbf{U}_w$ is the displacement vector of the wheelset. $\mathbf{U}_{bc}$ is the displacement vector of the contact point of the bridge/track-bridge system. $\mathbf{U}_s$ is the rail displacement correction vector. $\Delta\mathbf{U}$ is the penetration depth vector of the wheelset. $\mathbf{R}$ is the track irregularity vector. Equation (2) is the final wheel/rail constraint equation.

2.4. Iteration Convergence Criterion. The key point of the TTB interaction simulation is the compatibility of the force and the displacement between subsystems. In the FMT calculation process, the force satisfies Newton's third law and always maintains the force compatibility, while the displacement coordination must be iterated and updated step by step. In this paper, the Newton algorithm is chosen to update the displacement of the wheelset and the entire stiffness matrix.

The symbol $\boldsymbol{\psi}$ denotes the displacement difference vector between the train subsystem and track-bridge subsystem in the current iteration, which can be obtained from equation (2) as follows:

$$\boldsymbol{\psi} = \mathbf{U}_{bc} + \Delta\mathbf{U} + \mathbf{U}_s + \mathbf{R} - \mathbf{U}_w. \tag{3}$$

The input wheelset's displacement $\mathbf{U}_w$ determines the contact force between the wheel and rail. The contact force causes the nodal displacement of the track-bridge system. The nodal displacement of the track-bridge system is used to obtain the contact point displacement on the bridge $\mathbf{U}_{bc}$ via shape function interpolation. Thus, $\mathbf{U}_{bc}$ is also a function of the wheelset's displacement $\mathbf{U}_w$, notated as $\mathbf{U}_{bc} = g(\mathbf{U}_w)$. Similarly, the wheelset's penetration depth $\Delta\mathbf{U}$ is also a function of the wheelset's displacement $\mathbf{U}_w$, notated as $\Delta\mathbf{U} = h(\mathbf{U}_w)$. Substituting above both expressions into equation (3) results in

$$\boldsymbol{\psi} = g(\mathbf{U}_w) + h(\mathbf{U}_w) + \mathbf{U}_s + \mathbf{R} - \mathbf{U}_w. \tag{4}$$

By deriving the partial derivative of eqaution (4) with respect to each component of $\mathbf{U}_w$, the partial derivative of $\boldsymbol{\psi}'$ is given as follows:

$$\boldsymbol{\psi}' = \frac{\partial g(\mathbf{U}_w)}{\partial u_i} + \frac{\partial h(\mathbf{U}_w)}{\partial u_i} - \mathbf{I}, \tag{5}$$

where $\mathbf{I}$ denotes a unit matrix whose diagonal is one. u_i $(i = 1, \ldots, 4)$ denotes the displacement component of the ith wheelset. $\boldsymbol{\psi}'$ can be regarded as the equivalent tangent stiffness matrix. Note that the track irregularity vector $\mathbf{R}$ and the displacement correction vector $\mathbf{U}_s$ are constant in the above derivation process.

In the above numerical calculation process, the equivalent tangent stiffness matrix $\boldsymbol{\psi}'$ is calculated by the perturbation method. After obtaining $\boldsymbol{\psi}'$, according to the Newton update law, as shown in Figure 3, the new forced wheelset displacement of the next calculation step is given as follows:

$$\mathbf{U}_w^{k+1} = \mathbf{U}_w^k - [\boldsymbol{\psi}']^{-1} \cdot \boldsymbol{\psi}^k. \tag{6}$$

The convergence criterion of the wheel-rail displacement coordination is set as

$$|\boldsymbol{\psi}| \le \text{tol} = 10^{-8}\ \text{m}, \tag{7}$$

where tol is the convergence limit for the wheel-rail displacement coordination, and here tol is assumed to 10^{-8} m.

2.5. Calculation Flow Chart of the Convergence Estimation in FMT. This section will summarize the calculation flow chart of the convergence estimation in FMT. The detailed iteration process of each calculation step is shown in Figure 4 and is described as below.

Step 1: take out the given track irregularity vector $\mathbf{R}_n$ and extract the wheelset displacement vector $\mathbf{U}_w^{n,1}$ from the results of *No.* n time step, where n is an integer and $n \ge 1$. While $n = 1$ indicates the initial iteration, and $\mathbf{U}_w^{1,1}$ is an assumed suitable nonzero vector.

Step 2: apply $\mathbf{U}_w^{n,k}$ to the wheelset, in which superscript k denotes the iteration time and $k \ge 1$. Then, the train server performs dynamic analysis to obtain the contact force vector $\mathbf{F}_c^{n,k}$ on the wheelset.

Step 3: reverse the sign of $\mathbf{F}_c^{n,k}$, and then exert it on the track-bridge substructure. Then the track-bridge server

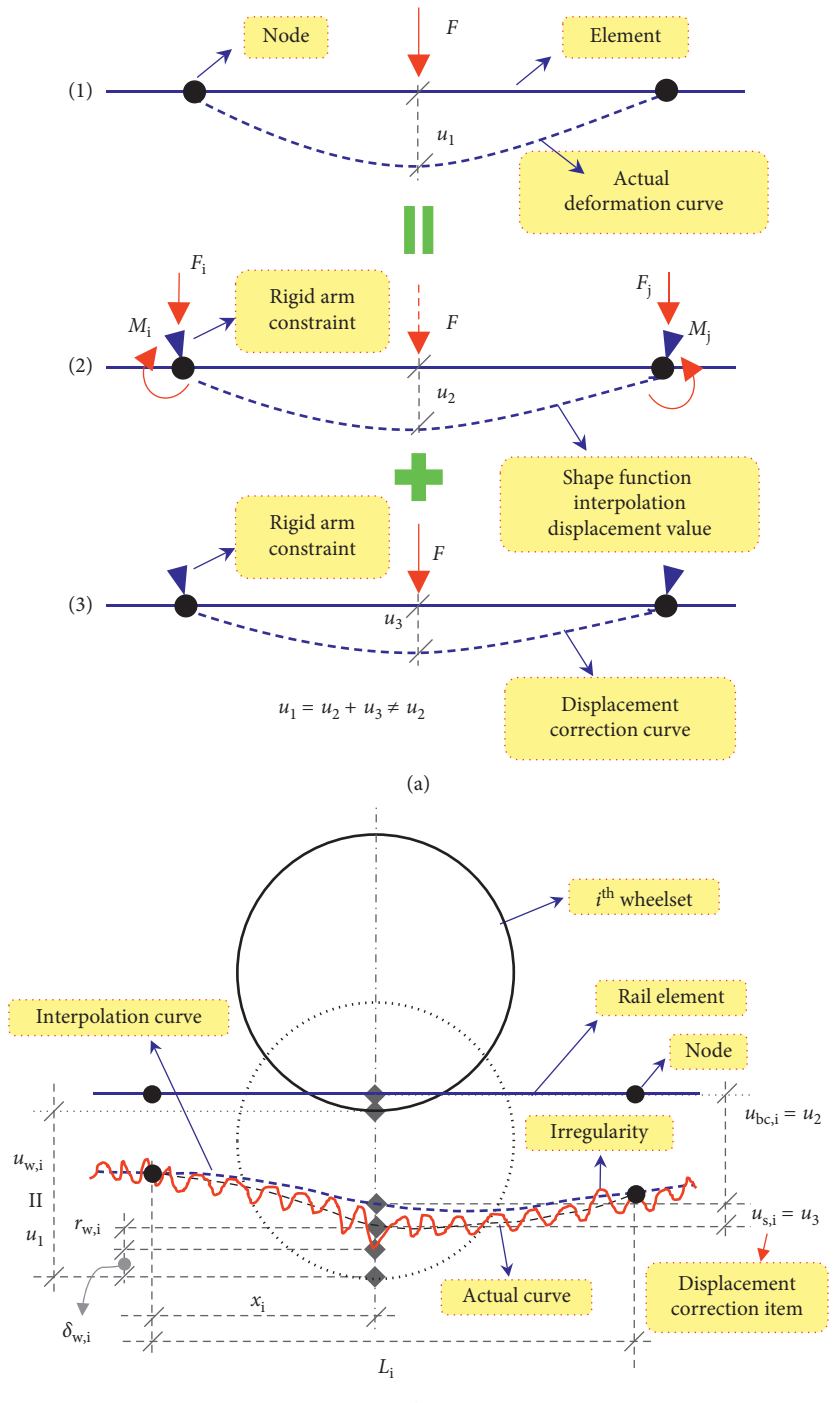

FIGURE 2: Diagram of wheel/rail constraint relationship. (a) Diagram of beam deformation subjected to a concentrated force. (b) Diagram of the geometrical relationship between wheel and rail.

performs dynamic analysis to get the nodal displacement vector $\mathbf{U}_b^{n,k}$ of the track-bridge.

Step 4: pass $\mathbf{U}_b^{n,k}$ to the client program. Then, the client calculates the contact point displacement on the bridge, $\mathbf{U}_{bc}^{n,k}$, by interpolating the bridge nodal displacement, $\mathbf{U}_b^{n,k}$, with shape function.

Step 5: according to equation (3), the client determines whether or not $\mathbf{U}_w^{n,k}$ and $\mathbf{U}_{bc}^{n,k}$ meet the displacement coordination condition in the current iteration. If *Not*, go to Step 6; if *Yes*, jump to Step 8.

Step 6: use the Newton update law to calculate new wheelset displacement $\mathbf{U}_w^{n,k+1}$ according to the equation (6).

Step 7: pass the new $\mathbf{U}_w^{n,k+1}$ to $\mathbf{U}_w^{n,k}$, and then repeat Step 2 to Step 7.

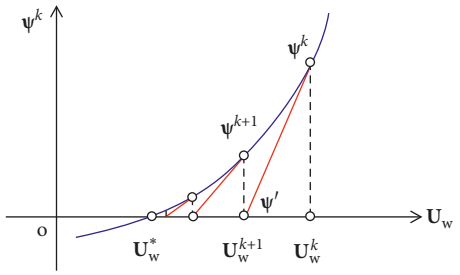

FIGURE 3: Displacement update based on the Newton update law.

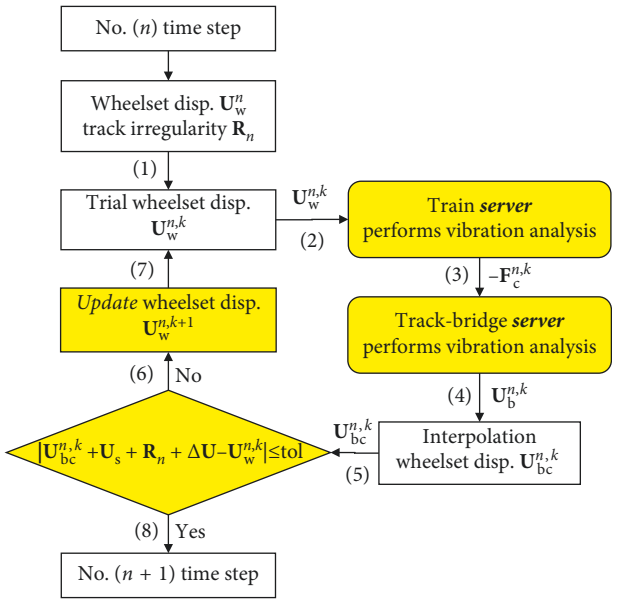

FIGURE 4: Flow chart of the convergence estimation in FMT.

Step 8: commit current state data and do the next loop for the *No.* $n+1$ time step.

3. Numerical Examples

3.1. Single-Wheel Vehicle over the Simply Supported Beam. Firstly, a classical single-wheel vehicle moving on a simply supported beam model [30] is simulated to calibrate the proposed method because this model has analytical solutions [10] and a well-recognized numerical solution [30]. The vehicle is represented as a lumped sprung mass and wheel is simulated with a very small mass. Among them, the vehicle and wheel are connected by a spring, and the effect of damping is neglected. In this model, the vehicle moves at a constant speed. The model and detailed parameters are shown in Figure 5.

The analysis results are shown in Figure 6. Compared with the literature, the acceleration response of the bridge's midspan has the same sine trend in three methods. While the fluctuation of three methods is different, Yang's solutions and the proposed FMT have the same order of magnitude of fluctuation, and both are greater than the fluctuation of analytical solution, which is a smooth sine trend, and are shown the Figure 6(a). This difference occurs because

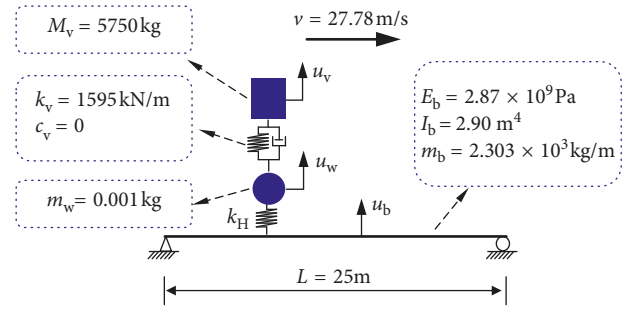

FIGURE 5: Moving single-wheel vehicle over a simply supported beam.

analytical solutions consider only the first-mode influence and ignore the corresponding higher-order mode effect. The ignored modes smoothen the sinusoidal variation of the bridge acceleration response and cause the responses of the train acceleration to differ slightly from the results of Yang's and the proposed method, as shown in Figure 6(b). Moreover, Yang's model ignores the effect of the Hertzian spring between the wheel and rail, so the fluctuation is smaller than the results of the proposed method. Thus, the analysis results illustrate that the proposed FMT technique is accurate and reliable.

3.2. Double Suspension Train over 10-Span Simply Supported Bridge. In this section, the FMT will be used to simulate a double suspension four-wheelset train moving over a 10-span simply supported bridge (SSB) model, as shown in Figure 7. The length per SSB is 32 m, and the total length of the model is 420 m, which includes 50 m of transition sections on both sides. And the purpose of the transition section is to ensure that the train is running smoothly when it enters the bridge. The track and bridge are connected by discrete springs and dampers with a 0.65 m interval. At both endpoints of SSB, the values of stiffness and damping parameters are half. The train is modeled as a multiple rigid body with the double suspension system and has 10 total DOFs, which include the vertical bouncing motion of the wheelset, the vertical bouncing, and pitch motion of both rigid body and bogies. The detailed parameters of the model are shown in Table 1. The train travels at a constant speed v = 27.78 m/s, and the calculation time step is 0.005 s. The point A is located in the middle of the fifth span of 10-span SSB model.

The entire numerical model is also built with OpenSees. The car body and bogie are simulated using the elasticBeamColumn element with sufficient bending stiffness to be equivalent to a rigid train; the rail and bridge are simulated using the dispBeamColumn element. And the spring and damper are simulated using the truss element.

This paper deals with the wheel-rail contact by a separating contact model, which means $\delta_{w,i}$ should be greater than and equal to zero. And the numerical integration scheme can be selected according to the requirements of the model in OpenSees, such as the Newmark-β method, Hilber-Hughes-Taylor method, and generalized alpha method [28];

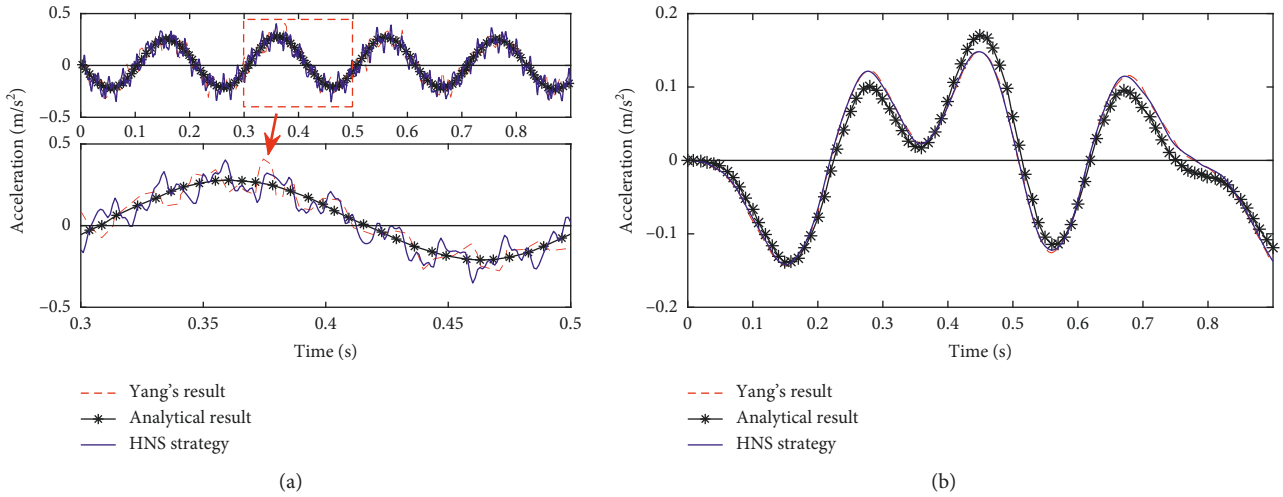

FIGURE 6: Time history responses of the bridge and the train. (a) Acceleration responses of the bridge's midpoint. (b) Acceleration responses of the car body.

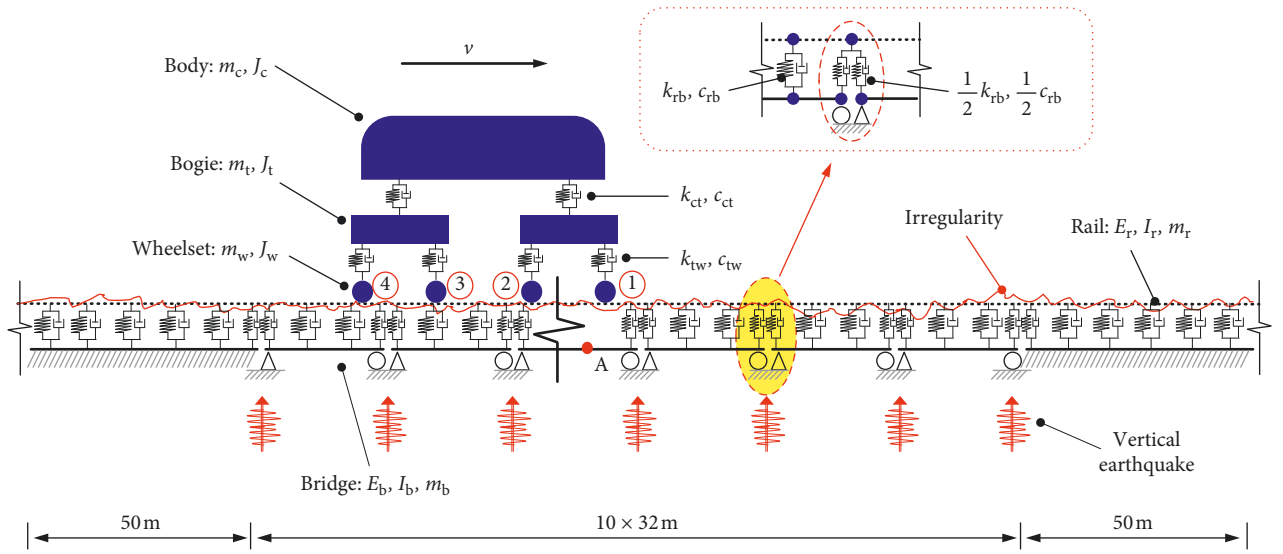

FIGURE 7: Finite element model of the train-track-bridge system under earthquake.

this is one of the advantages of the proposed FMT technique. In this model, the Newmark-β method difference scheme is adopted.

This section will use the above model to analyze different situations, i.e., comparison of computational efficiency of different methods, the displacement correction effect, the nonlinear second suspension effect, and the Tabas earthquake excitation. The detailed cases' values are listed in Table 2.

3.2.1. Comparison of Computational Efficiency and Iteration Times of Different Methods. In this subsection, the computational efficiency of SCA, LCA, and FMT will be compared. Liu et al. [15] summarized the commonly used TTB analysis methods to strongly coupled algorithms (SCA) and loosely coupled algorithms (LCA). The SCA considers the train, track, and bridge as a single integrated system, while the LCA considers the train, track, and bridge as the separated system. In order to compare the calculation efficiency with FMT, we program the SCA and LCA methods with the MATLAB and use them to analyze the 10-span SSB model. Then, the calculated results and the computational efficiency are compared.

In this example, the track irregularity excitation is always present. The SCA and LCA just take into account the linear second spring suspension effect of the train, while the FMT considers the linear and nonlinear second spring suspension effect of the train; for the nonlinear curve, refer to Figure 8(a). The results are shown in Figure 9, the acceleration response of the train body of FMT linear is basically consistent with those of SCA and LCA, while the result of FMT nonlinear case is slightly larger than the other three cases. The reason may be that the initial stiffness of the nonlinear suspension spring is less than that of the linear

Table 1: The model parameters.

Parameter	Notation	Value	Unit
Bridge			
Length per single	L_b	32	m
Young's modulus	E_b	$2.94E+10$	Pa
Moment inertia	I_b	$5.0E+5$	m^4
Mass density per unit length	m_b	$5.0E+5$	kg/m
Track			
Young's modulus	E_r	$2.06E+11$	Pa
Moment inertia	I_r	$4.07E-5$	m^4
Mass density per unit length	m_r	103	kg/m
Connection stiffness between rail and bridge	k_{rb}	$1.32E+8$	N/m
Connection damping between rail and bridge	c_{rb}	$6.42E+4$	N·s/m
Train			
Train body mass	m_c	$5.20E+4$	kg
Roll mass moment of train body	J_c	$2.31E+6$	kg·m^2
Bogie mass	m_{bg}	3200.00	kg
Roll mass moment of bogie	J_{bg}	3120.00	kg·m^2
Wheelset mass	m_w	1400.00	kg
Stiffness of second suspension	k_{ct}	$1.72E+6$	N/m
Damping of second suspension	c_{ct}	$1.96E+5$	N·s/m
Stiffness of primary suspension	k_{tw}	$1.87E+6$	N/m
Damping of primary suspension	c_{tw}	$5.00E+5$	N·s/m
Half distance of two bogies	L_c	9.00	m
Half distance of two wheelsets	L_t	1.25	m

Table 2: The case table.

Case number	1	2	3	4	5	6	7	9
Displacement correction	×	✓	✓	✓	✓	✓	✓	✓
Nonlinear second suspension	×	×	✓	✓	✓	✓	✓	✓
Track irregularity	×	×	×	×	✓	✓	✓	✓
Tabas earthquake	×	×	×	×	✓	✓	✓	✓
Intensity (g)/Comments			Damper	Spring	0.05 g	0.10 g	0.20 g	0.40 g

Note. × means not to consider the item, and ✓ means to consider the item. Case 3 considers the second nonlinear damper, and case 4 considers the second nonlinear spring.

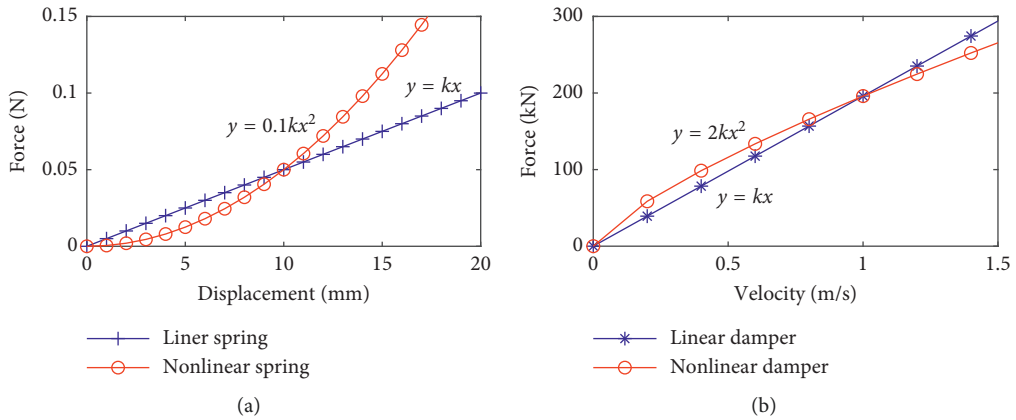

Figure 8: The second nonlinear suspension characteristics. (a) Nonlinear spring curve (case 3). (b) Nonlinear damper curve (case 4).

suspension spring. The comparison of elapsed time and iterations is listed in Table 3. In the linear case, the FMT's time consumption is a little more than the SCA and LCA, and the maximal iteration of FMT is the same as one of LCA and is 3. In the nonlinear case, the FMT's time consumption increased by about 20% than the linear case. Meanwhile, the maximal iteration was raised to 5.

In summary, the FMT has no advantage in computational efficiency, but it is efficient in modeling and nonlinear situation.

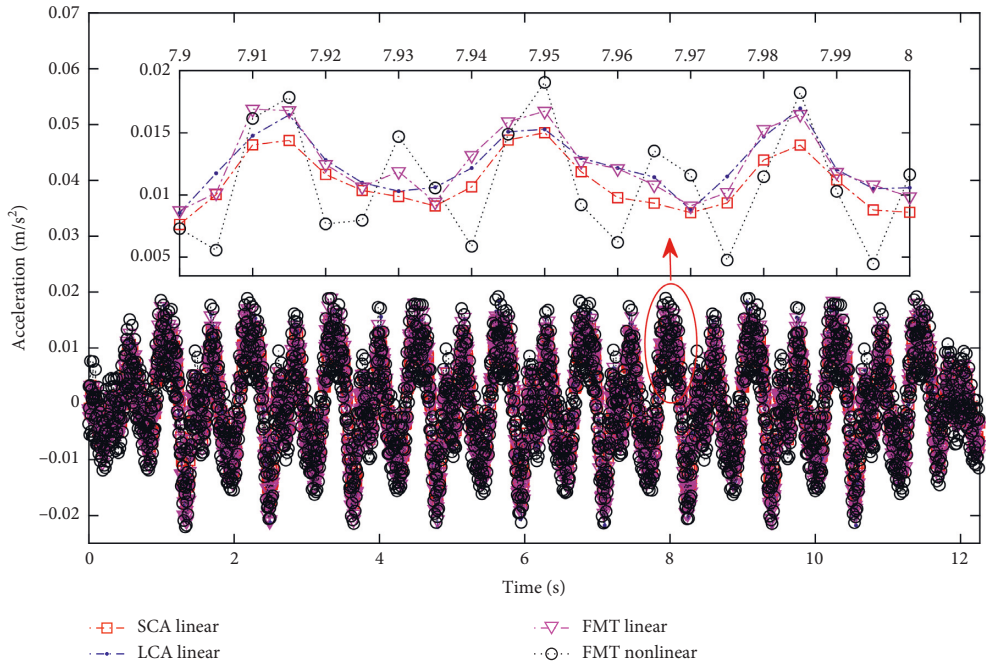

Figure 9: Comparison diagram of car body acceleration response with different methods.

Table 3: Elapsed time and iterations of the methods.

Method	Cases	Time (s)	Max iteration
SCA	Linear model	1287	0
LCA	Linear model	1670	3
FMT	Linear model	1770	3
FMT	Nonlinear model	2112	5

3.2.2. Displacement Correction Effect. In this section, the effect of the rail displacement correction (DC) is compared between cases 1 and 2 in Table 2. Case 1 considers only the moving train load effect, and case 2 includes the effect of DC. The moment when the first wheelset contacts the bridge is regarded as time zero. The analysis results are shown in Figure 10 and Table 4.

Figure 10(a) and Table 4 demonstrate that DC will increase the wheel/rail contact forces. Table 4 shows that the maximum and minimum values of the DAF effect percentage are 3.7862, and −3.8052, respectively. Hence, the DC will increase or decrease the wheel/rail contact force by approximately 4%. Figures 10(c) and 10(d) illustrate that the effect of DC on the acceleration of the train body is relatively small. Overall, DC will reduce the body's acceleration response, especially at high frequencies above approximately 35 Hz. The reason may be that the track structure becomes soft when considering the DC effect, so the high-frequency response of the train is more difficult to determine. Figure 10(b) shows that the DC has less influence on the bridge's displacement response; the bridge's acceleration response, the displacement, and acceleration responses of the track have the same phenomenon and small variations.

Hence, in summary, the displacement correction (DC) has little effect on the track and bridge structures, but it has an impact on the wheel/rail contact forces and reduces the train body acceleration response at high frequencies.

3.2.3. Nonlinear Suspension Effect. In this section, the nonlinear suspension characteristics are investigated. It includes the nonlinearity of the damper and spring of the second suspension. Both curves are shown in Figure 8. For the curve form, refer to Garg's book [31].

Figure 11(a) shows that the nonlinear second damper will increase the train body acceleration response, while the nonlinear second spring has little effect on the body acceleration response. Figure 11(b) indicates that the train body's displacement amplitude of the linear and nonlinear damper and nonlinear spring of the second suspension is 0.70, 0.77, and 0.76 mm, respectively. The train body's vibration amplitude of the linear and nonlinear damper and nonlinear spring of the second suspension is 0.30 mm, 0.28 mm, and 0.35 mm, respectively. Consequently, the results show that the displacement vibration response of the train body will be decreased by the nonlinear second damper and increased by the nonlinear second spring. The acceleration amplitude of the train body will be increased by both.

The reason is possible that the nonlinear spring reduces the stiffness under small deformation, which results in a larger vibration amplitude than the linear case, while the nonlinear damper increases the damping under small velocities, which results in a smaller vibration amplitude than the linear case.

Figure 12 shows that both the nonlinear second damper and spring suspension have a little influence on the contact forces and displacement response of the bridge.

In sum, the nonlinear suspension affects only the train system and has no effect on the supported system and the

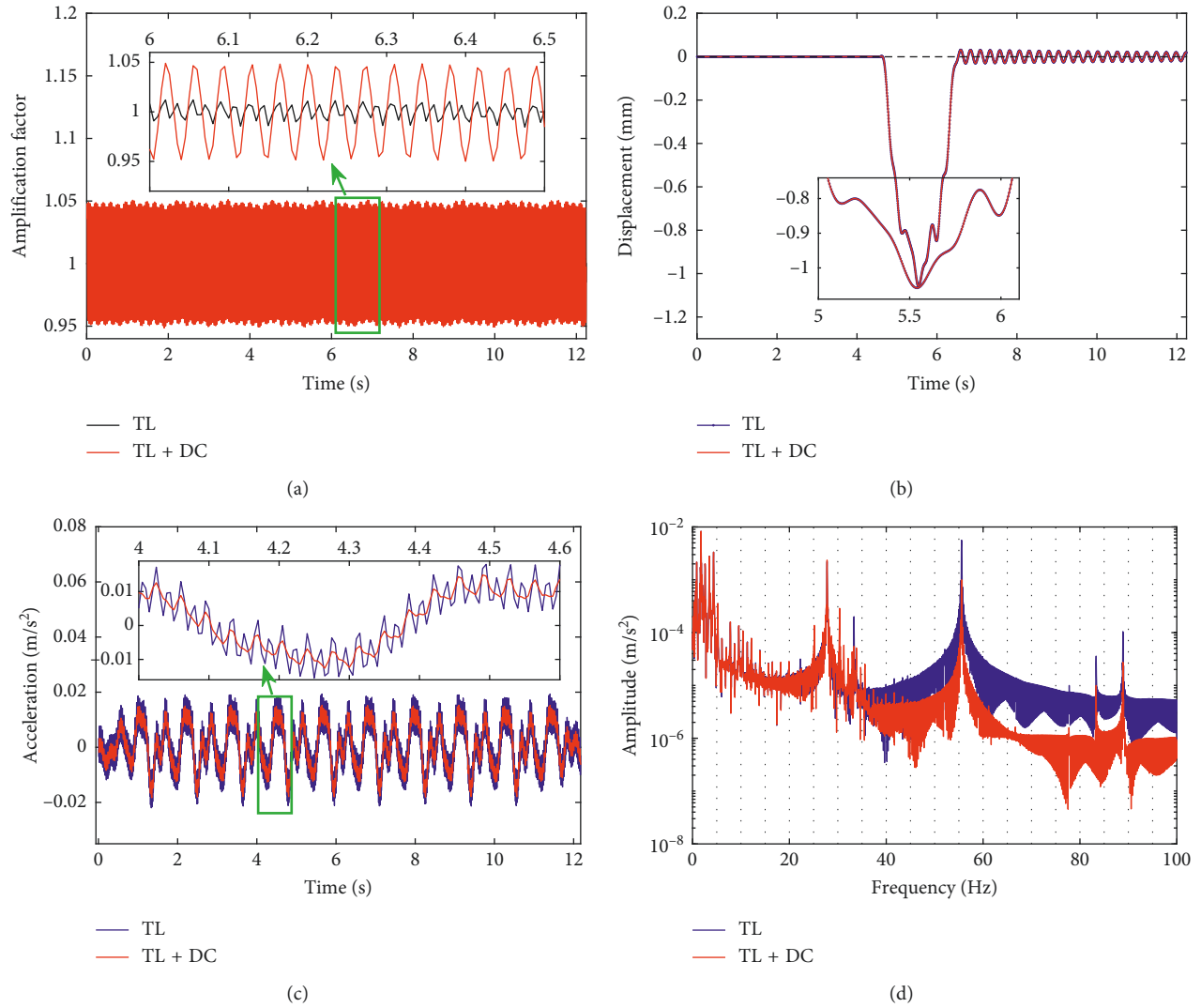

Figure 10: The typical responses of the train and bridge. (a) Dynamic amplification factors of the first wheelset. (b) Displacement response of point A. (c) Car body acceleration time history response. (d) The Fourier transform of train body acceleration.

Table 4: Dynamic amplification factors of the wheel-rail contact forces.

Cases		(1) TL	(2) TL + DC	((2)-(1))/(1) (%) percentage of DC effect
1st wheelset	Max DAF	1.0132	1.0511	3.7406
	Min DAF	0.9834	0.9486	−3.5387
2nd wheelset	Max DAF	1.0142	1.0526	3.7862
	Min DAF	0.9855	0.9480	−3.8052
3rd wheelset	Max DAF	1.0126	1.0503	3.7231
	Min DAF	0.9837	0.9490	−3.5275
4th wheelset	Max DAF	1.0137	1.0518	3.7585
	Min DAF	0.9856	0.9482	−3.7946

TL: train load; DC: displacement correction; DAF: dynamic amplification factors. The minus sign means wheel-rail contact forces reduction.

contact forces. In addition, adjusting the second suspension damper is more effective than adjusting the second suspension spring to improve operational comfort of the train.

3.2.4. Earthquake Excitation Effect. In this section, the response of the TTB systems subjected to a vertical Tabas earthquake is investigated. The original Tabas earthquake record is shown in Figure 13. According to the Chinese Seismic Code [27], the acceleration amplitudes of earthquake records are adjusted to the corresponding intensity, as shown in Table 2.

The acceleration and displacement responses of the train are shown in Figure 14 and Table 5. Compared to the case

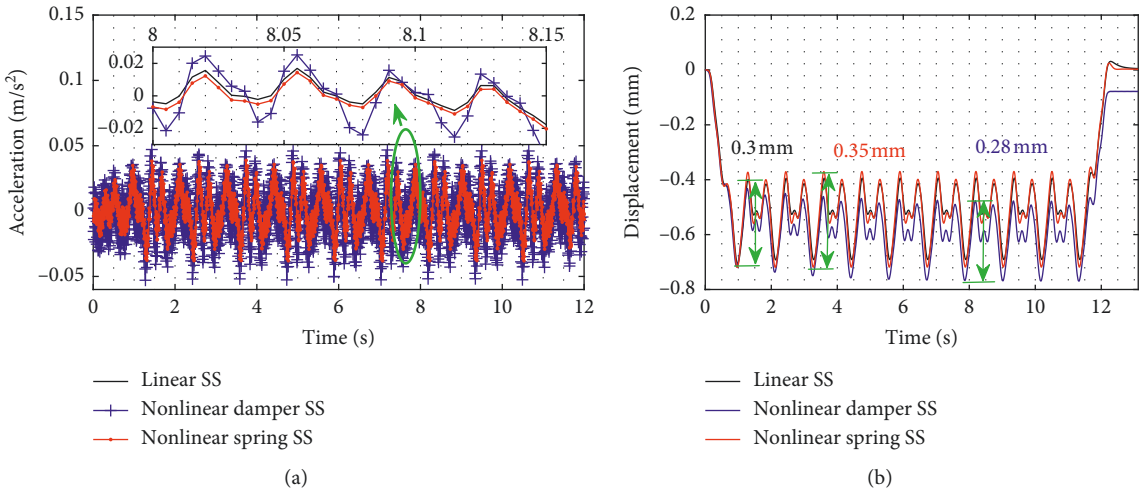

Figure 11: Train body responses considering nonlinear second suspension (note: SS = second suspension). (a) Car body acceleration response. (b) Car body displacement response.

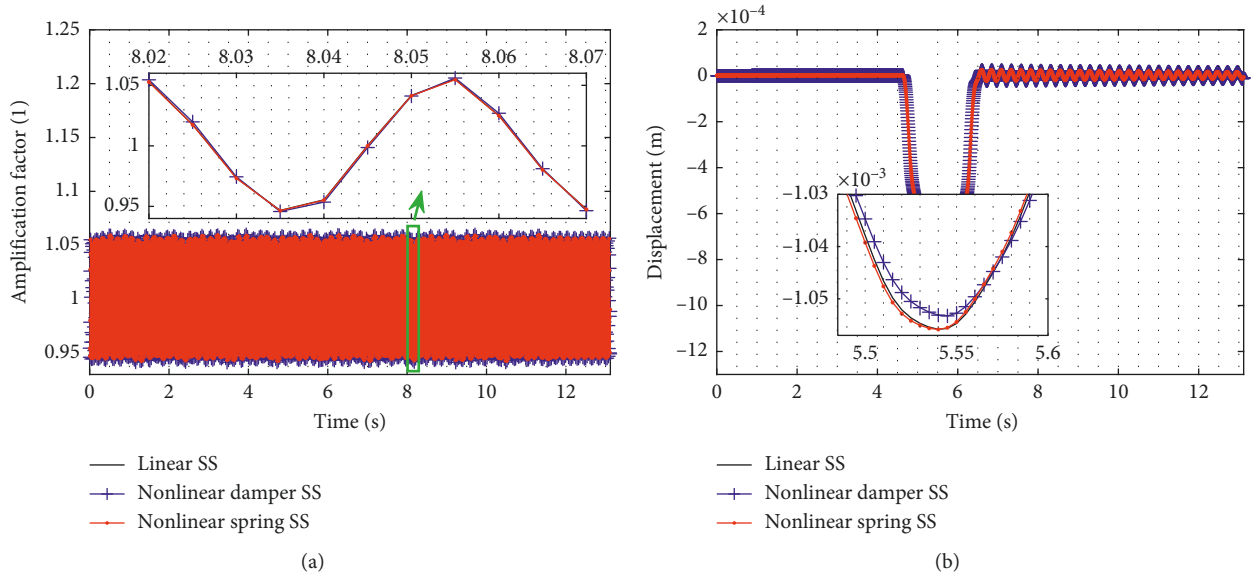

Figure 12: The contact forces and bridge displacement responses under nonlinear second suspension (note that the 5th bridge means the fifth bridge between the total 10-span simply supported beam bridge model). (a) Amplification factor of contact forces. (b) Bridge displacement response of point A.

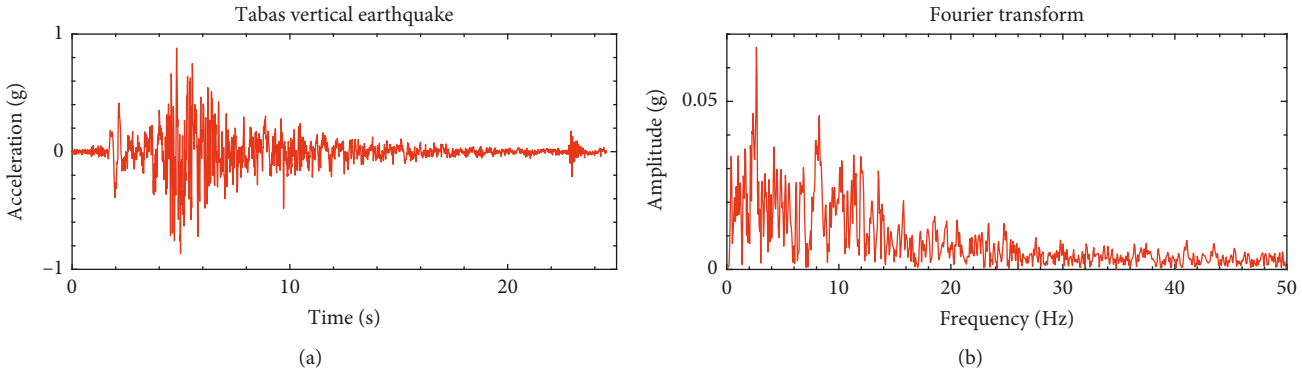

Figure 13: The Tabas earthquake records. (a) Tabas acceleration time history. (b) Fourier transform of acceleration.

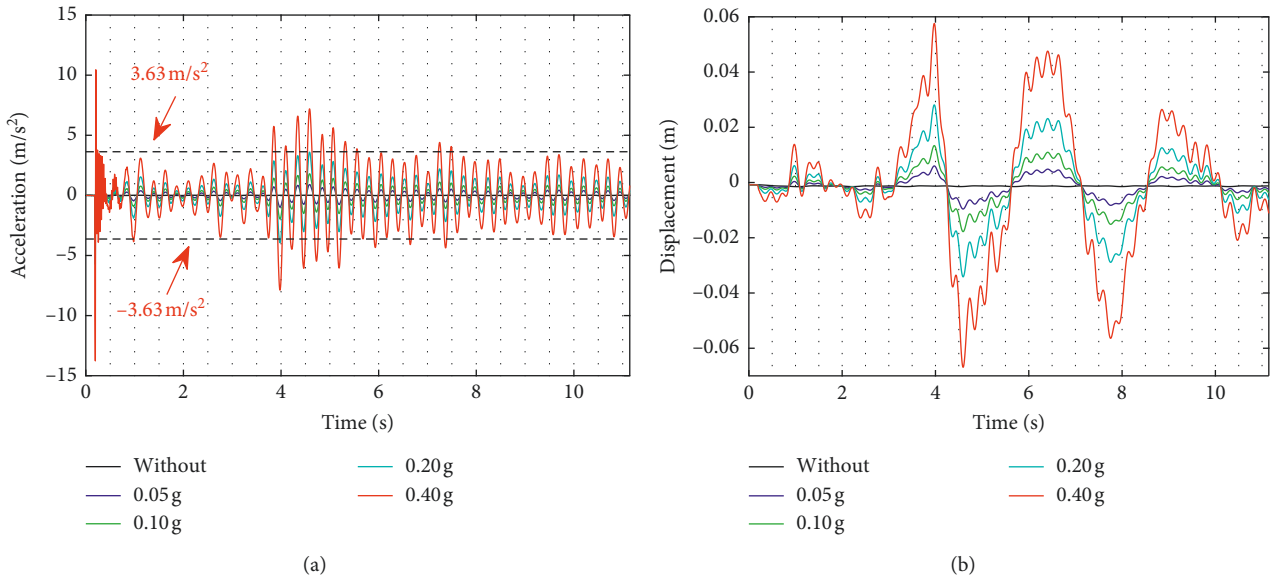

Figure 14: Seismic response of the car body at 100 km/h. (a) Body acceleration. (b) Body relative displacement.

Table 5: Dynamic responses of the train's body peak acceleration and peak displacement.

Cases		(I) 0.00 g	(II) 0.05 g	(III) 0.10 g	(IV) 0.20 g	(V) 0.40 g
Body peak acceleration (g)	A^i_{max}	0.0193	0.8981	1.7981	3.5983	10.4473
	A^i_{min}	−0.0220	−1.2455	−2.4743	−5.7381	−13.7650
	$(\mathrm{Max}(\lvert A^i_{max}\rvert, \lvert A^i_{min}\rvert))/\lvert A^I_{max}\rvert$	1.00	64.39	127.92	296.67	711.66
Body peak displacement (m)	D^i_{max}	−0.0008	0.0060	0.0134	0.0281	0.0576
	D^i_{min}	−0.0015	−0.0096	−0.0178	−0.0341	−0.0669
	$\mathrm{Max}(\lvert D^i_{max}\rvert, \lvert D^i_{min}\rvert)/\lvert D^I_{max}\rvert$	1.00	12.58	23.31	44.78	87.73

DE: the design earthquake.

without an earthquake excitation, the acceleration and displacement responses of the car body increase as the earthquake intensity increases. As shown in Table 5, the maximum acceleration is amplified 64.39 times, and the displacement amplitude is amplified by 12.58 times under an earthquake acceleration amplitude of 0.05 g, which is the common seismic fortification intensity in China. According to the Chinese Code [32], one of the train stability acceptance criteria is that the train body vertical acceleration must be less than 3.63 m/s^2. Figure 14(a) shows that when the acceleration exceeds 0.2 g, the car body vertical acceleration exceeds the stability criteria. Thus, considering the Tabas seismic wave, may be the train operation is not safe when the earthquake intensity exceeds 0.10 g at a speed of 100 km/h. The displacement amplification factors are smaller than the acceleration amplification factors for all records, which means the body acceleration is more sensitive to earthquakes than body displacement. The acceleration and displacement responses of the rail and the bridge also display the same phenomenon.

The responses of the wheel/rail contact force are shown in Figure 15 and Table 6. The contact forces also increase as the earthquake intensity increases. The response of the train and bridge structure is significantly increased during an earthquake. When the acceleration of the earthquake excitation is adjusted to greater than or equal to 0.20 g, the contact forces have zero values, which means the wheelset will jump from the rail, and separation occurs. Meanwhile, the train stability index will exceed the criterion. So, the FMT could conveniently consider the wheel/rail separation phenomenon and the seismic excitation.

4. Conclusions

In this paper, a fast modeling technique (FMT) is proposed and used to simulate the train-track-bridge (TTB) systems. In detail, the FMT combines the train subsystem and the track-bridge subsystem via the client-server technique to perform the TTB coupling vibration analysis on simplex OpenSees simulation platform. One feature of FMT is easy to use for the junior researchers to analyze the TTB problem. And another feature of FMT is that it will significantly reduce the amount of data transmission between subsystems. Therefore, it can be directly utilized to dramatically reduce the time consumed during the building model and dealing with wheel/rail relation. In addition, this method could make full use of the OpenSees' advantages to performing the seismic analysis, nonlinear analysis, and wheel/rail separation

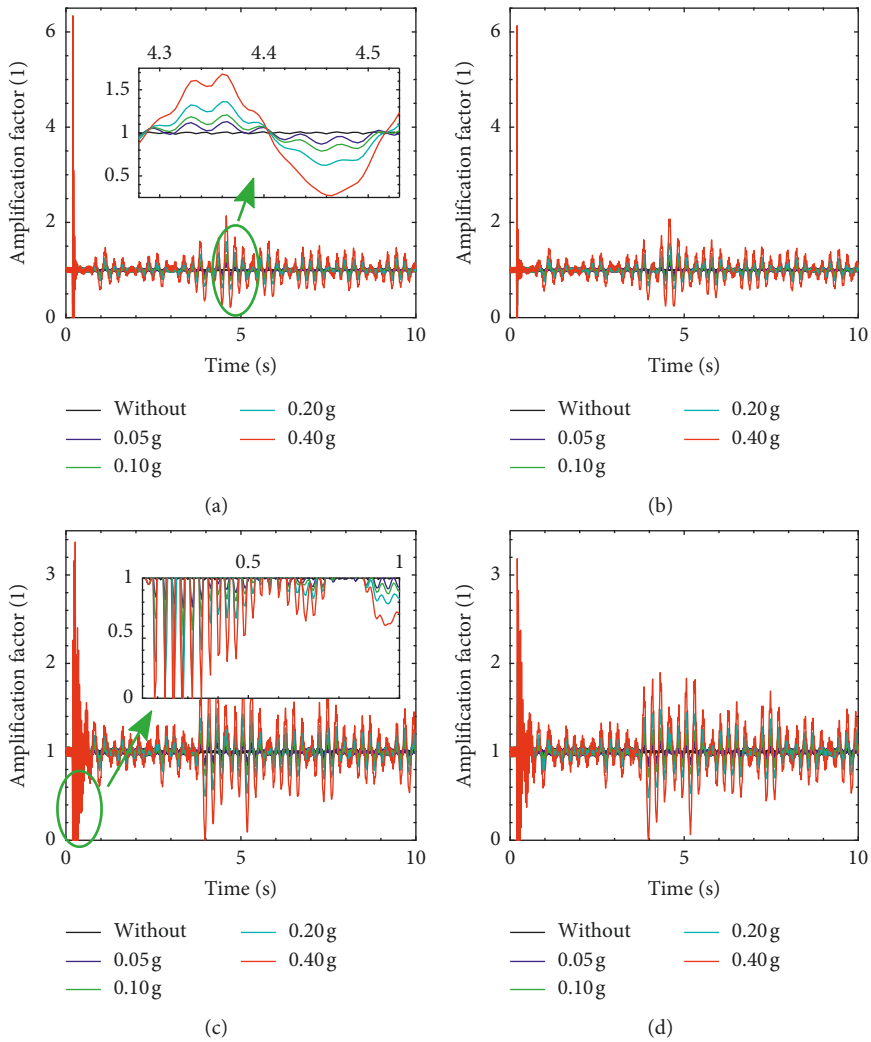

Figure 15: Wheel-rail contact force amplification factor. (a) 1st wheelset. (b) 2nd wheelset. (c) 3rd wheelset. (d) 4th wheelset.

Table 6: Dynamic acceleration amplification factors of wheel-track contact forces.

Cases		(I) 0.00 g	(II) 0.05 g	(III) 0.10 g	(IV) 0.20 g	(V) 0.40 g
1st wheelset	Max DAF	1.01	1.32	1.66	2.98	6.34
	Min DAF	0.98	0.67	0.28	0.00	0.00
2nd wheelset	Max DAF	1.01	1.32	1.62	3.03	6.13
	Min DAF	0.99	0.53	0.11	0.00	0.00
3rd wheelset	Max DAF	1.01	1.26	1.48	2.00	3.37
	Min DAF	0.98	0.75	0.52	0.00	0.00
4th wheelset	Max DAF	1.01	1.36	1.66	2.24	3.19
	Min DAF	0.99	0.57	0.20	0.00	0.00

DAF: dynamic amplification factors; DE: the design earthquake.

phenomenon for TTB systems. So, the FMT is a practical and suitable technique to simulate the TTB interaction, and it could improve the modeling efficiency to save time.

Data Availability

The data used to support the findings of this study are included within the article.

Conflicts of Interest

The authors declare that they have no conflicts of interest.

Acknowledgments

This work was financially supported by the High-Speed Rail Joint Fund (U1434204) and the National Natural Science Foundation of China (51778630 and 51878674).

References

[1] W. M. Zhai, H. Xia, C. B. Cai et al., "High-speed train-track-bridge dynamic interactions part I: theoretical model and numerical simulation," *International Journal of Rail Transportation*, vol. 1, no. 1-2, pp. 3–24, 2013.

[2] T. Arvidsson and R. Karoumi, "Train–bridge interaction—a review and discussion of key model parameters," *International Journal of Rail Transportation*, vol. 2, no. 3, pp. 147–186, 2014.

[3] Q. Gu, Y. D. Liu, W. Guo, W. Li, Z. Yu, and L. Jiang, "A practical wheel-rail interaction element for modeling vehicle-track-bridge systems," *International Journal of Structural Stability and Dynamics*, vol. 19, no. 2, article 1950011, 2018.

[4] W.-M. Zhai, "Two simple fast integration methods for large-scale dynamic problems in engineering," *International Journal for Numerical Methods in Engineering*, vol. 39, no. 24, pp. 4199–4214, 1996.

[5] W. M. Zhai, *Vehicle-Track Coupling Dynamics*, Science Press, Beijing, China, 2015.

[6] Z. Zhu, W. Gong, L. Wang, I. E. Harik, and Y. Bai, "A hybrid solution for studying vibrations of coupled train–track–bridge system," *Advances in Structural Engineering*, vol. 20, no. 11, pp. 1699–1711, 2017.

[7] Z. Zhu, W. Gong, L. Wang et al., "An efficient multi-time-step method for train-track-bridge interaction," *Computers & Structures*, vol. 196, pp. 36–48, 2018.

[8] Y. B. Yang, J. D. Yau, Z. D. Yao, and Y. S. Wu, *Vehicle-Bridge Interaction Dynamics: with Applications to High-Speed Railways*, World Scientific, Singapore, 2004.

[9] Y.-B. Yang and B.-H. Lin, "Vehicle-bridge interaction analysis by dynamic condensation method," *Journal of Structural Engineering*, vol. 121, no. 11, pp. 1636–1643, 1995.

[10] J. M. Biggs, *Introduction to Structural Dynamics*, McGraw-Hill College, New York, NY, USA, 1964.

[11] L. Fryba, *Vibration of Solids and Structures under Moving Loads*, Thomas Telford Ltd., London, UK, 3rd edition, 1999.

[12] H. Xia and N. Zhang, "Dynamic analysis of railway bridge under high-speed trains," *Computers and Structures*, vol. 83, no. 23-24, pp. 1891–1901, 2005.

[13] M. Olsson, "Finite element, modal co-ordinate analysis of structures subjected to moving loads," *Journal of Sound and Vibration*, vol. 99, no. 1, pp. 1–12, 1985.

[14] S. C. Yang and S. H. Hwang, "Train-track-bridge interaction by coupling direct stiffness method and mode superposition method," *Journal of Bridge Engineering*, vol. 21, no. 10, article 04016058, 2016.

[15] K. Liu, N. Zhang, H. Xia, and G. De Roeck, "A comparison of different solution algorithms for the numerical analysis of vehicle-bridge interaction," *International Journal of Structural Stability and Dynamics*, vol. 14, no. 2, article 1350065, 2014.

[16] S.-H. Ju and H.-T. Lin, "Numerical investigation of a steel arch bridge and interaction with high-speed trains," *Engineering Structures*, vol. 25, no. 2, pp. 241–250, 2003.

[17] H. Xia, N. Zhang, and R. Gao, "Experimental analysis of railway bridge under high-speed trains," *Journal of Sound and Vibration*, vol. 282, no. 1-2, pp. 517–528, 2005.

[18] C. H. Lee, M. Kawatani, C. W. Kim, N. Nishimura, and Y. Kobayashi, "Dynamic response of a monorail steel bridge under a moving train," *Journal of Sound and Vibration*, vol. 294, no. 3, pp. 562–579, 2006.

[19] F. Yang and G. A. Fonder, "An iterative solution method for dynamic response of bridge-vehicles systems," *Earthquake Engineering & Structural Dynamics*, vol. 25, no. 2, pp. 195–215, 1996.

[20] J. W. Kwark, E. S. Choi, Y. J. Kim, B. S. Kim, and S. I. Kim, "Dynamic behavior of two-span continuous concrete bridges under moving high-speed train," *Computers and Structures*, vol. 82, no. 4-5, pp. 463–474, 2004.

[21] S. Cui, *Coupled vibration simulation analysis of vehicle-bridge system based on multi-body system dynamics and finite element method*, Ph.D. dissertation, Southwest Jiaotong University, Chengdu, China, 2009.

[22] Y. Li, X. Xu, Y. Zhou et al., "An interactive method for the analysis of the simulation of vehicle-bridge coupling vibration using ANSYS and SIMPACK," *Proceedings of the Institution of Mechanical Engineers, Part F: Journal of Rail and Rapid Transit*, vol. 232, no. 3, pp. 663–679, 2018.

[23] J. Auciello, E. Meli, S. Falomi, and M. Malvezzi, "Dynamic simulation of railway vehicles: wheel/rail contact analysis," *Vehicle System Dynamics*, vol. 47, no. 7, pp. 867–899, 2009.

[24] W. Hou, Y. Li, W. Guo, J. Li, Y. Chen, and X. Duan, "Railway vehicle induced vibration energy harvesting and saving of rail transit segmental prefabricated and assembling bridges," *Journal of Cleaner Production*, vol. 182, pp. 946–959, 2018.

[25] Q. Gu and O. Ozcelik, "Integrating OpenSees with other software—with application to coupling problems in civil engineering," *Structural Engineering and Mechanics*, vol. 40, no. 1, pp. 85–103, 2011.

[26] F. T. McKenna, *Object-oriented finite element programming frameworks for analysis, algorithms and parallel computing*, Ph.D. dissertation, University of California, Berkeley, CA, USA, 1997.

[27] GB 5001-2010 Code, *Code for Seismic Design of Buildings*, China Architectural and Building Press, Beijing, China, 2010.

[28] OpenSees official website, http://opensees.berkeley.edu/wiki/index.php/Modeling_Commands.

[29] P. Lou, "Finite element analysis for train–track–bridge interaction system," *Archive of Applied Mechanics*, vol. 77, no. 10, pp. 707–728, 2007.

[30] Y.-B. Yang and Y.-S. Wu, "A versatile element for analyzing vehicle-bridge interaction response," *Engineering Structures*, vol. 23, no. 5, pp. 452–469, 2001.

[31] V. K. Garg and R. V. Dukkipati, *Dynamic of Railway Vehicle Systems*, Elsevier, Amsterdam, Netherlands, 1984.

[32] TB/T 2360-93 Code, *The Identification Method and Evaluation Standard for Dynamic Performance Test of Railway Locomotives*, Ministry of Railways of PRC, Beijing, China, 1993.

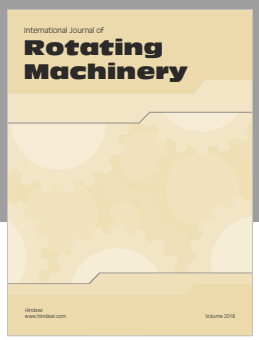

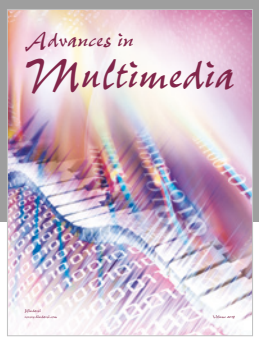

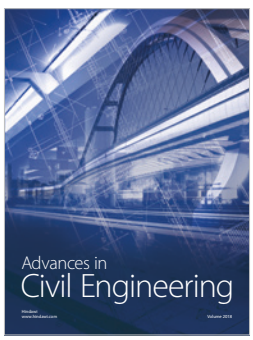

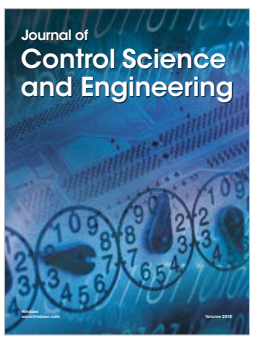

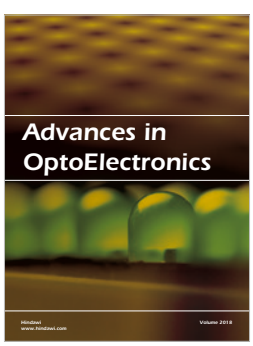

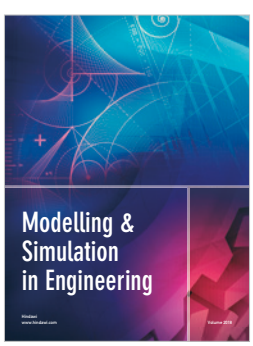

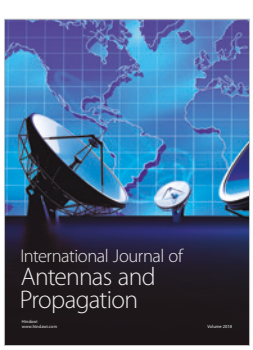

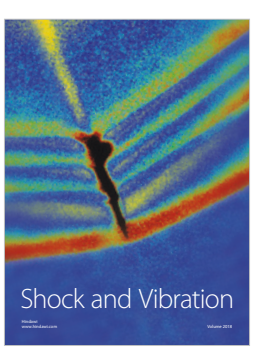

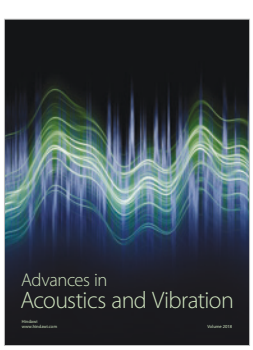

Hindawi

Submit your manuscripts at
www.hindawi.com